

Castor Oil and PEG-Based Shape Memory Polyurethane Films for Biomedical Applications

Mirey Bonfil,¹ Ahmet Sirkecioglu,¹ Ozlem Bingol-Ozakupinar,² Fikriye Uras,² F. Seniha Güner¹

¹Department of Chemical Engineering, Istanbul Technical University, Maslak 34469 Istanbul, Turkey

²Department of Biochemistry, Marmara University, Faculty of Pharmacy, Tibbiye Cad. No 49, Haydarpasa 34668 Istanbul, Turkey

Correspondence to: F. S. Guner (E-mail: guners@itu.edu.tr)

ABSTRACT: A series of polyurethane film were prepared from poly(ethylene glycol) with different molecular weight (PEG 1500, 3000, and 8000) and castor oil by one-shot bulk polymerization method. Hexamethylene diisocyanate and 1,4-buthane diol were used as diisocyanate and chain extender, respectively. In order to characterize the samples, their density, swelling ratio, water contact angle, surface free energy, gel content, thermal, and viscoelastic properties were determined. The effect of the soft segment length (SSL) and hard segment content (HSC) of all polyurethane films on their shape memory behavior such as shape fixity (R_f) and shape recovery (R_r) rates were investigated by bending test. Direct contact and MTT tests were used for assessment of cell adhesion and proliferation. The relatively high R_f and R_r values were obtained for the samples programmed at high temperature difference. R_f increased with decreasing HSC. On the other hand, R_r tended to decrease with increasing SSL. After evaluating experimental data by a nonlinear equation, it was found that HSC is more effective parameter on shape memory property than SSL. The gel content, swelling ratio, and water contact angle of the samples were dependent on both SSL and HSC in their structures. © 2014 Wiley Periodicals, Inc. *J. Appl. Polym. Sci.* **2014**, *131*, 40590.

KEYWORDS: biomaterials; polyurethanes; properties and characterization

Received 8 October 2013; accepted 6 February 2014

DOI: 10.1002/app.40590

INTRODUCTION

Shape memory polymers (SMPs) are smart materials that have the ability to return from a deformed state (temporary shape) to their original shape induced by an external effect.¹ The external effect can be thermal heating, electric field, magnetic field, light, etc. The commonly used effect is thermal heating due to the simplicity for setting. A thermosensitive shape memory polymer has a capability to recover its temporary shape to original shape above a transition temperature which is glass transition temperature or melting temperature.

Shape memory polyurethanes (SMPUs) are one of the most typical thermo-sensitive SMPs, which were extensively studied in the near past decades. A segmented SMPU has two phases (hard and soft segments) on its structures, and these segments cause phase separation. The crystalline part of polyurethane occurs in soft segment which forms reversible phase and also, it determines the shape recovery temperature.^{2–4} Soft segment absorbs the energy of external effect and keeps the material elastic at low temperature. On the other hand, the hard segment composes the frozen phase. Hydrogen bonding and dipole–dipole interaction hold hard segments together, thus original

shape of the polymer is recovered on heating above the transition temperature. In brief, the performance of a SMPU is especially related to its chemical structure such as hard segment content (HSC), soft segment length (SSL), degree of hydrogen bonding, etc.^{5,6} Additionally, programming or shape-holding conditions also define the shape memory properties of polyurethanes.⁷

For the sake of sustainability, renewable sources are widely used as raw material for various applications. Among them, triglyceride oils are one of the most valuable renewable sources used for polymer preparation.^{8,9} In literature, oil based-SMPs were synthesized from a variety of oils and different aspects of their behaviors were investigated. For example, soybean oil-based-SMPs were successfully prepared, and their properties were investigated in relation to the chemical stoichiometry and the oil properties.¹⁰ It is reported that shape memory properties are closely related to the crosslinking densities and glass transition temperatures of the polymers. In other study, biocompatible and biodegradable porous castor oil based-polyurethane was synthesized via sol–gel chemistry by Lippincott.¹¹ Additionally, amorphous or semicrystalline thermoset polyurethane networks were synthesized from castor oil based-polyols using ADMET

chemistry by Rio et al.¹² They pointed out that semicrystalline polyurethane exhibits good shape memory properties.

Depending on the application, a SMP should have some properties. From a biomedical point of view, it is important to produce biodegradable and biocompatible SMP which has a high shape recovery rate at human body temperature.^{1,13,14} The main goal of this study is to prepare shape memory polyurethane films for tailored transition temperature close to human body temperature. For this purpose, two of the most important parameters which are polyurethane composition and programming conditions, were investigated. First catalyst- and solvent-free synthesis of polyurethane was achieved from polyethylene glycol (PEG) and castor oil with varying HSC and SSL. Then their shape memory properties were determined by bending test with two different cooling rates in programming step, and the influence of HSC, SSL, and cooling rate on shape memory properties were investigated. In order to explain the polymer behavior, the influence of HSC and SSL on some polymer properties such as density, swelling ratio, water contact angle, surface free energy, gel content, thermal, and viscoelastic properties were also investigated.

EXPERIMENTAL

Materials

Castor oil (CO) with hydroxyl number 161.01 mg KOH/g and acid number 0.99 mg KOH/g was supplied by Sorel Chemicals. Polyethylene glycol (PEG) with a molecular weight of 1500, 3000 or 8000 from Fluka and 1,6-hexamethylene diisocyanate (HDI) from Merck (analytical grade) were used in polymer synthesis. Also, 1,4-buthane diol (BDO) from Fluka was used as a chain extender.

Polymer Synthesis

Polyurethanes were prepared by one-step bulk polymerization technique. PEG was dried on a rotary evaporator for 6 h at 90–95°C and CO was dried at 80°C under vacuum for 24 h. BDO was dried overnight at 50°C in a vacuum oven.

PEG and/or CO was added into a flask and mixed. Then, BDO (5.7% by weight) were added into the flask and mixed until obtaining a homogeneous mixture. The mixture poured into a three-necked reaction flask equipped with a mechanical stirrer, dropping funnel and N₂ inlet and outlet. After heating the reaction mixture to 50°C, HDI was added to the mixture at the stirring rate of 300 rpm. After 150 s, the reaction mixture was poured into the molds and placed in an oven at 80°C. HDI was used in an amount such that the equivalent ratio of isocyanate groups to hydroxyl groups. The reaction was monitored by Fourier transform infrared (FTIR) spectroscopy. The disappearance of the absorption peak at 2250 cm⁻¹, assigned to the N=C=O group, confirmed that all the diisocyanate was consumed in the reaction. This was usually achieved in about 20 h. The average functionality (*f*) of CO was calculated to be 2.67, using eq. (1).

$$\frac{MW}{f} = \frac{56100}{HV} \quad (1)$$

where MW and HV are molecular weight (=932 g/mol) and hydroxyl value (=161.01 mg KOH/g sample) of CO, respectively.

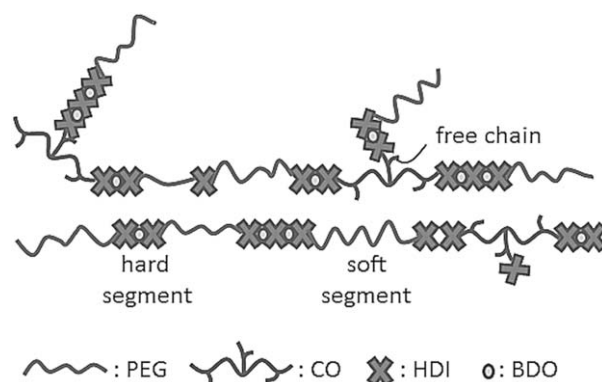


Figure 1. Schematic representation of polyurethane structure.

A schematic representation of polymer structure for the polyurethane synthesized from PEG, CO, and HDI is given in Figure 1. Samples were designated by using the abbreviation PU-*a-b*, where *a* indicates the molecular weight of PEG, and *b* indicates the CO percentage in CO and PEG mixture.

Polymer Characterization

FTIR spectra were obtained using a Perkin Elmer Spectrum One instrument. The thermal gravimetric analysis (TGA) studies were carried out using a Perkin Elmer Diomand TGA, by heating from room temperature to 550°C, under nitrogen atmosphere with a heating rate of 20°C/min. The differential scanning calorimeter (DSC) measurements were carried out on a Perkin Elmer Diamond DSC at the temperature ranging from -60 to 200°C with a heating rate of 10°C/min. The viscoelastic properties of polymer films were determined by Perkin Elmer Diamond DMA operating in tensile mode. The relaxation spectrum was scanned from -60 to 80°C with a frequency of 1 Hz and with a heating rate of 2°C/min. The crystallinity of polymer films was determined by using wide angle X-ray scattering, and calculated from the ratio of diffraction peak area and total diffraction area.¹⁵

Swelling ratio was determined by immersing polymer into distilled water at 37°C until equilibrium was reached, and determined gravimetrically by weighing the water saturated polymers after removing excess water from the polymer surfaces with a paper towel. Static contact angle and surface free energy measurements were conducted using KSV CAM200 goniometer by placing 5 μL of distilled water on the polymer surface. Gel content of the polymer was determined with Soxhlet extractor using acetone as solvent. Density of the polymer was determined at room temperature by Precisa balance XB 620 M.

Crosslink Density and Average Molecular Weight Between Two Crosslinks

Crosslink density (*v_c*) and average molecular weight between two crosslinks (*M_c*) were determined by two methods; the equilibrium swelling method according to the Flory-Rehner equation¹⁶ and the rubber elasticity method using DMA curves.¹⁷

Equation (2) was used to calculate *M_c* in the equilibrium swelling method. Toluene was the solvent chosen for all the polymers in the calculations.

$$M_C = \frac{v_s d_p (V_p^{1/3} - V_p/2)}{\ln(1 - V_p) + V_p + \chi_{12} V_p^2} \quad (2)$$

where v_s is the molar volume of the solvent, V_p is the volume fraction of the polymer in the swollen state, and χ_{12} is the polymer–solvent interaction parameter of the solvent, which can be estimated by eq. (3).

$$\chi_{12} = 0.34 + \frac{v_s (\delta_p - \delta_s)^2}{RT} \quad (3)$$

where δ_p and δ_s are the solubility parameters of the polymer and solvent, respectively. Solubility parameters of the polymers were determined by swelling experiment. Measurements were performed at 25°C. Polymers were swollen to equilibrium in several solvents such as toluene, acetone, 1,4-dioxane, n-methyl-2-pyrrolidone, and methanol. Their solubility parameters are 8.9, 9.9, 10, 11, and 14.5 (cal/cm³)^{1/2},¹⁶ respectively. The equilibrium degree of swelling (Q) calculated according to eqs. (4) and (5) was plotted against the solubility parameters of the solvents.

$$V_p = \frac{W_p/d_p}{W_p/d_p + W_s/d_s} \quad (4)$$

$$Q = \frac{1}{V_p} \quad (5)$$

where W_p is dry weight of polymer, W_s is weight of the solvent, d_p is the density of the polymer, and d_s is density of solvent.

For calculation M_c by rubber elasticity method the value of the storage modulus (E') at the rubbery plateau (20°C) was used in eq. (6).¹⁷

$$M_C = d_p \frac{3RT}{E'} \quad (6)$$

where R is the gas constant and T is the absolute temperature (K). Equation (7) was used for calculation of v_c in both the equilibrium swelling and the rubber elasticity methods.

$$v_c = \frac{d_p}{M_C} \quad (7)$$

Shape Memory Property

Bending test was used to determine the shape memory property (Figure 2).¹⁸ A band of sample with a dimension of 5 cm × 1.5 cm × 0.1 cm was cut and the test was applied in three different procedures. In the first procedure, the sample was heated to 65°C for 5 min and deformed to an angle θ_{\max} under force. Then, the deformed sample was cooled to 25°C for 5 min, the force released, and the angle was remeasured and recorded as a θ_{fixed} . By being heated to 65°C for 5 min in oven, the sample was recovered its original shape and the final angle reached after recovery was measured, θ_{final} . In the second procedure, similar steps of the first procedure were followed except the cooling step. In the cooling step, the sample was cooled from 65°C to 5°C in an ice bath, and so the test was performed at relatively high cooling rate. To simulate the performance of the samples in human body the third test was applied. For this purpose, the samples were deformed as in the second procedure and shape

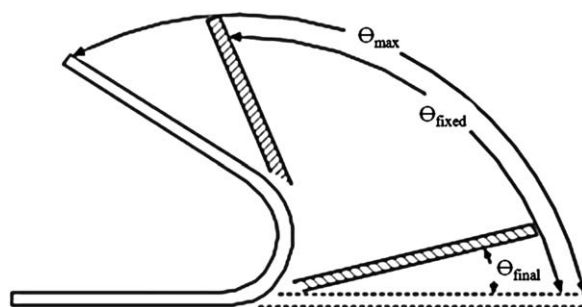


Figure 2. Illustration of bending test method.

recovery rate of all samples was determined at 37°C in phosphate buffer solution (PBS).

In all tests, shape fixity rate (R_f) and shape recovery rate (R_r) were calculated via the eqs. (8) and (9). To test reusability of the polyurethanes as shape memory materials, shape recovery, and shape fixity tests were repeated six times for each polymer in various batch and the average of the results were calculated. In order to determine reusability of a sample, its shape memory behavior was determined in six consecutive measurements by bending test.

$$R_f = \frac{\theta_{\text{fixed}}}{\theta_{\max}} \times 100 \quad (8)$$

$$R_r = \left(\frac{\theta_{\text{fixed}} - \theta_{\text{final}}}{\theta_{\text{fixed}}} \right) \times 100 \quad (9)$$

Cell Culture and Cytotoxicity of Polyurethane Films

Circular discs of 6 mm-diameter per sample were cut and then they were sterilized for 30 min in 70% ethanol containing 150 U/mL antibiotics under UV light and then washed with PBS twice. Two methods were used for assessment of cell adhesion and proliferation; direct contact and 3-(4,5-dimethylthiazol-2-yl)-2,5-diphenyltetrazolium bromide (MTT) tests.

In the direct contact test, murine fibroblast NIH 3T3 cell line (seeding density 5000 per well) was precultured for 24 h in Dulbecco's modified essential medium (DMEM) supplemented with bovine serum (10%) in tissue culture plates and then exposed for 24 h to the polymers placed in the center of each well in a humidified atmosphere (e.g., 37°C, 5.0% CO₂). The morphological changes indicating cytotoxicity and cell growth characteristics were observed using an inverted microscope (Olympus, Tokyo, Japan). Wells containing cells but no polymer were used as control.

In MTT, cells were allowed to attach for 24 h in the presence of individual polymers, then the medium was removed and 100 μ L of growth medium with MTT (5 mg/mL in PBS) was added to the wells. MTT was converted to blue formazan crystals by intact mitochondrial reductase during a 4 h contact period. The medium was then removed and the precipitated crystals were dissolved in 100 μ L of the solubilization buffer consisting of SDS-HCl. Finally, the reduced MTT was measured at 545 nm using a microplate reader. Wells containing cells but no polymer (positive control) were used to evaluate the effects of the polymers. Wells containing polymer but no cells were used as a

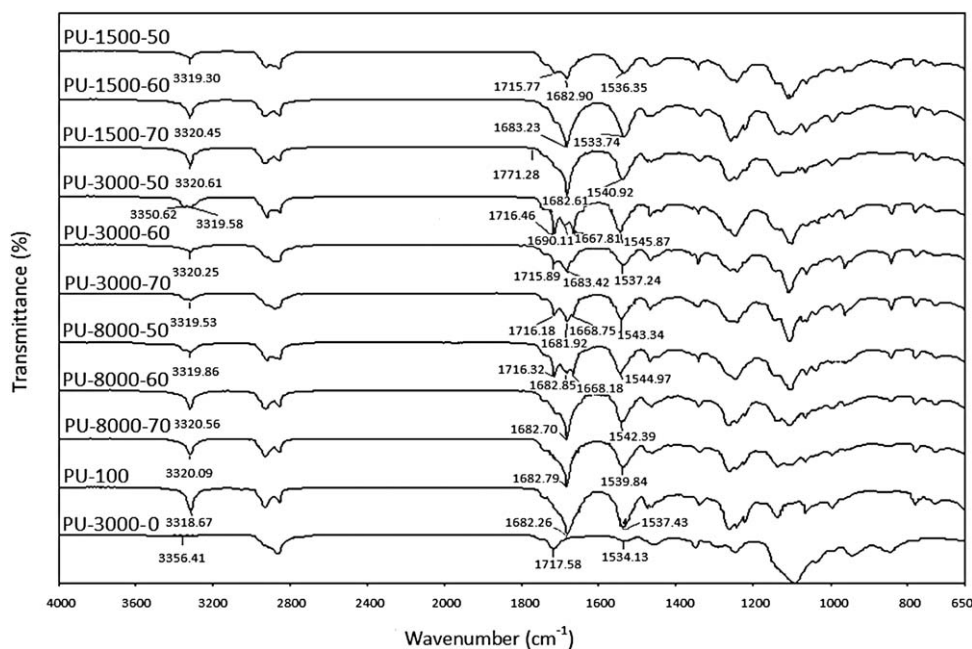


Figure 3. FTIR spectra of polyurethane films.

negative control. Reported values are the mean of three replicates and are expressed as percentages of the positive control values.

RESULTS AND DISCUSSION

In order to investigate the effects of the soft segment length (SSL), the hard segment content (HSC), and the crosslink density on some polymer properties including shape memory property, the polyurethanes were synthesized with a varying ratio of CO to PEG from different molecular weight of PEG. HSC was adjusted in polymer structure by the weight ratio of CO to PEG, and it was calculated as the total weight ratio of CO, HDI, and BDO to all reactants. The molecular weight of PEG was assumed as the SSL of polymer.

Polymer Synthesis and Characterization

All samples exhibit characteristic polyurethane peaks in their FTIR spectra (Figure 3). As mentioned in experimental part, the absence of the absorbance at around 2265 cm^{-1} for the final product indicated consuming of isocyanates and formation of polyurethane.¹⁹ The disappearance of the absorption peak at 3464 cm^{-1} , assigned to the hydroxyl group, confirmed that all hydroxyl groups were consumed in the reaction. CO is an ester product of glycerol and ricinoleic acid, and hence the CO-based polyurethane chains include ester bonds besides urethane bonds. The peak around 1740 cm^{-1} is attributed to the carbonyl stretching of the ester group.

Two main regions are widely investigated for evaluation of FTIR spectrum of polyurethanes. They are amide (N—H) stretching vibration ($3200\text{--}3500\text{ cm}^{-1}$) and carbonyl (C=O) stretching vibration in amide I ($1650\text{--}1760\text{ cm}^{-1}$) regions.²⁰ Hydrogen-bonded urethane C=O and N—H vibration peaks appear around 1660 cm^{-1} and 3320 cm^{-1} , respectively. All samples exhibit characteristic polyurethane peaks in their FTIR spectra

(Figure 3). FTIR spectra for two regions of all polyurethanes prepared in this study are shown in Figures 5 and 6. In order to evaluate FTIR spectrums of the samples, two polyurethanes were also synthesized from castor oil (PU-100) and PEG3000 (PU-3000-0). PU-100 was synthesized without PEG and PU-3000-0 was prepared without CO. Their spectrums are also added in Figures 3–5.

In the NH stretching region, two peaks are dominant at around 3320 and 3350 cm^{-1} for the polyurethanes prepared from both PEG and CO. On the other hand, the polyurethane based on only CO (PU-100) showed a strong peak at around 3316 cm^{-1} , whereas polyurethane based on only PEG3000 (PU-3000-0) gave a peak at around 3354 cm^{-1} . According to these results, the peaks at around 3320 and 3350 cm^{-1} were proposed for the samples prepared from both PEG and CO, belong to vibration of H-bonded NH for ester and ether structures, respectively. Similar explanation is given by Karak et al.²¹ The absence of a peak at around 3500 cm^{-1} indicates that there are no free NH groups in polyurethane structures. If there are, their concentration is below detection limit.

In the carbonyl stretching vibration in amide I region, a strong peak was obtained at 1717 cm^{-1} for the sample based on only PEG3000 (PU-3000-0). This indicates the presence of H-bonded urethane C=O groups for ether structure. In the case of polyurethane based on only castor oil (PU-100), a strong peak was determined at around 1682 cm^{-1} . This peak indicates the presence of H-bonded urethane C=O groups for ester structure. For the samples prepared from both PEG and castor oil, these two peaks were observed in various intensities. The intensity of the peak at 1682 cm^{-1} decreased with decreasing the ratio of CO to PEG, since the amount of ester carbonyl decreased in polymer structure. The strong peak was determined for PU-8000-50, PU-3000-50, and PU-3000-70 at around 1716 cm^{-1} due to relatively high molecular weight PEG and low ratio of

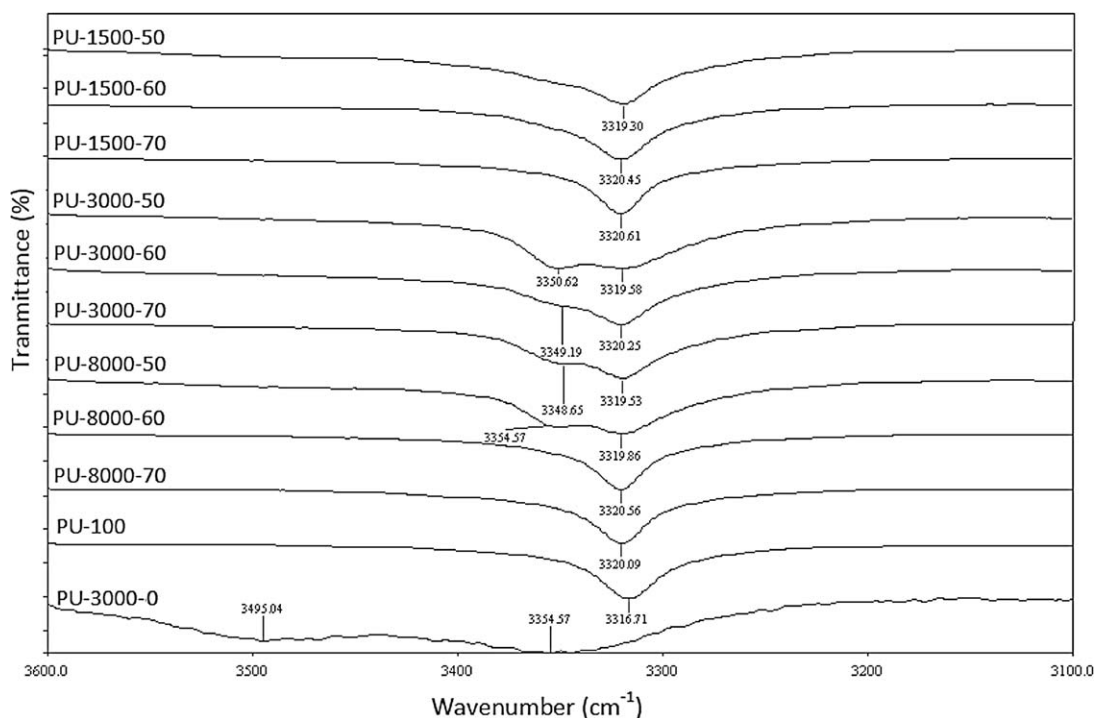


Figure 4. FTIR spectra for NH stretching regions of polyurethane films.

CO to PEG. Expected results were obtained for PU-8000-50 and PU-3000-50. As compared the samples according to the molecular weight of PEG used in their synthesis, they were synthesized from the highest two molecular weight of PEG, and additionally, the amount of PEG in polymer structure was relatively high. Unexpected result was obtained for PU-3000-70. Although the amount of PEG is the smallest in its structure among the

polymers prepared in the study, the intensity of the peak indicating H-bonded urethane carbonyl groups for ether structure was relatively high. This may be due to effect of crosslinks. Since the amount of castor oil was relatively high in polymer structure, the polymer chains got close to each other, and so, H-bonds may occur between NH groups and urethane carbonyl groups for ether structure. Nevertheless, Oprea reported that

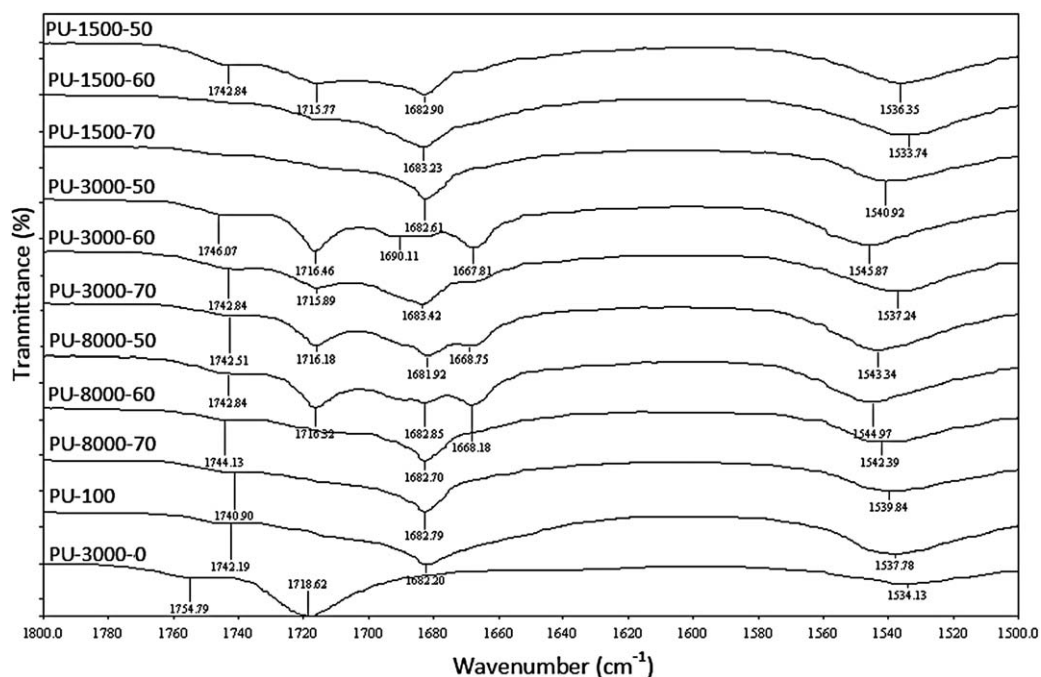


Figure 5. FTIR spectra for C=O stretching regions of polyurethane films.

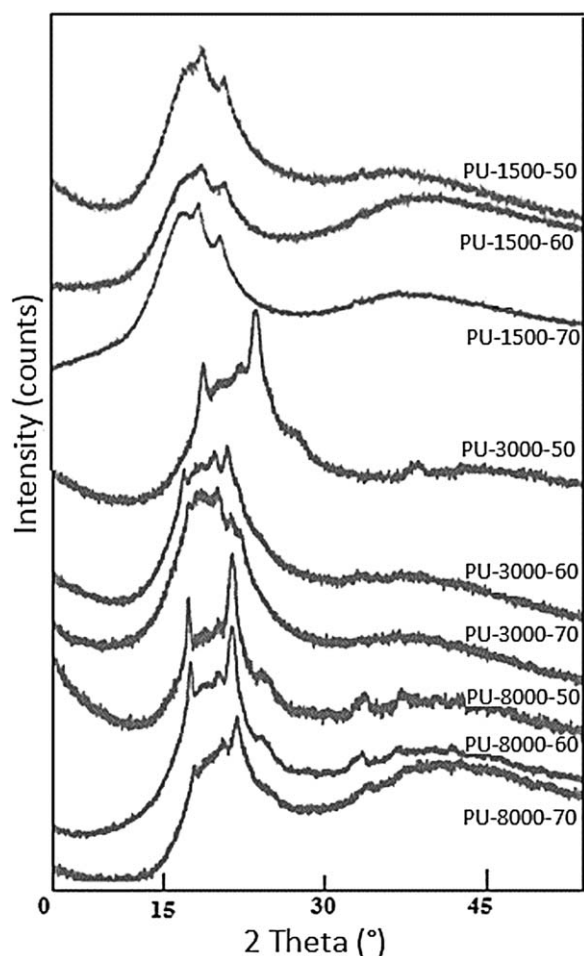


Figure 6. X-ray diffraction patterns of polyurethane films.

due to steric hindrance of dangling chains coming from castor oil, the formation of hydrogen bonding was blocked in polyurethane structure.²²

The evidences obtained from the region in the $1535\text{--}1545\text{ cm}^{-1}$ confirmed the results discussed above. The infrared band observed in the spectrum of all samples in this region indicates the N—H bending vibration in the amide II region. The peak shifts from 1545 cm^{-1} to $1535\text{--}1537\text{ cm}^{-1}$ for the PU-1500-50 and PU-3000-60-coded polyurethanes. The similar trend was also observed for PU-100 and PU-3000-0. The shift to lower frequency is an indication of the weakening of the hydrogen bonds.²³

As mentioned in literature,²⁴ the free carbonyl peak coming from castor oil appeared around 1743 cm^{-1} for all samples, except PU-3000-0.

X-ray diffraction patterns of the polyurethanes are shown in Figure 6. The PU-3000-50, PU-8000-50, and PU-8000-60 samples exhibited some sharp peaks at around $2\theta = 18\text{--}23^\circ$, characteristic of PEG crystallinity. There are also the characteristic peaks of PEG in the X-ray pattern of other samples, but these are not strong. Degree of crystallinity for each polyurethane sample was calculated from XRD data (Table I). As expected, crystallinity of the polymers increased by decreasing castor oil

content and increasing molecular weight of PEG. The crystallinity of all samples was also determined from DSC data discussed in the following section.

Thermal and Viscoelastic Properties

Since the TGA thermogram of a sample is overlapped with others, a few TGA thermograms are presented in Figure 7(a,b) for showing the trends. All samples decomposed in two steps. The first and second degradation steps occurred between $300\text{--}400^\circ\text{C}$ and $400\text{--}500^\circ\text{C}$, respectively. It is well known that polyurethanes decompose in two²⁵ or three^{21,24} steps depending on the chemical structure of the hard and soft segments. Almost the same initial decomposition temperature (ca., 250°C) was observed for the samples. Two intersection points between TGA curves of the samples were observed at about 350 and 425°C . The decomposition temperatures of all samples in various weight losses are given in Table I.

Degree of crystallinity for polyurethane samples was also calculated from DSC data (Table I). For this purpose, the crystallinity was calculated from the ratio of the enthalpy of the samples (ΔH_m , Figure 8) and the enthalpy of melting of 100% crystalline PEG ($\Delta H_m(\text{PEG}) = 202.41\text{ J/g}$).²⁶ Again, crystallinity increased with increasing molecular weight and amount of PEG in polyurethane structure. The crystallinity calculated from XRD and DSC data were not the same, particularly for high crystallinity, but a similar trend was observed.

The crystalline melting temperature (T_m) was used as a transition temperature for shape memory behavior in this study. T_m for each polymer obtained from its DSC curve is given in Table I. As expected, T_m of polyurethanes increased with increasing SSL. For the PU-3000-coded polymers, T_m increased with decreasing HSC. Since the T_m value of PU-3000-50-coded polymer is close to the human body temperature, it is particularly suitable for biomedical applications. In literature, the importance of the transition temperature for biomedical applications is emphasized by Ahmad et al.¹⁴ Among several polyurethane-based SMPs, they proposed to use the samples having glass transition temperature (T_g) of $35\text{--}45^\circ\text{C}$ for medical devices, since their transition temperatures close enough to the body temperature.

Figures 9 and 10 show the dynamic mechanical behavior of all the prepared polyurethanes. All polymers exhibited two thermal transitions which are T_g at lower temperatures and the melting of crystalline domain of soft segment at the higher temperatures. T_g of polyurethanes shifted to higher temperature with increasing the molecular weight of PEG. T_g highly depended on SSL. Polyurethane prepared with higher molecular weight of PEG had higher T_g . On the other hand, CO:PEG ratio did not affect the T_g of polyurethanes. PU-3000-70-coded polyurethane showed wider plateau of storage modules (Figure 10) than the others, which shows a well-developed network structure. This might be due to the microphase separation between soft and hard segments. The glass transition temperatures (T_g) of all polyurethanes obtained from DMA measurements are below room temperature, consequently they are rubbery at human body temperature (Table II). The height of tan δ graph gives knowledge on chain mobility in polymer systems.²⁷ According to the

Table I. Crosslink Density and Average Molecular Weight Between Two Crosslinks of Polyurethane Films and Thermal Properties

Code	T_m (°C)	X_c (%) by:		T_g (°C) by:		$v_c \times 10^3$ (mol/cm ³) by:		M_c (g/mol) by:		Decomposition temperature determined by TGA at weight loss of;		
		XRD	DSC	DMA	DSC	DMA	Flory-Rehner	DMA	Flory-Rehner	10%	50%	90%
PU-1500-50	25.4	22.7	14.6	-41.3	-56.4	1.65	3.10	655	349	318	407	454
PU-1500-60	24.4	-	3.9	-33.2	-55.4	1.61	3.12	667	343	321	395	444
PU-1500-70	23.3	-	-	-36.7	-52.0	-	3.16	-	335	322	399	454
PU-3000-50	38.9	33.2	29.4	-24.5	-32.1	2.13	1.43	509	734	327	409	445
PU-3000-60	33.2	31.1	6.5	-24.7	-31.3	0.68	2.06	1574	520	3287	406	451
PU-3000-70	20.5	-	-	-25.5	-30.1	0.24	2.23	4386	466	327	400	453
PU-8000-50	51.4	37.0	27.7	-21.7	-26.0	4.61	0.96	232	1109	314	411	456
PU-8000-60	54.4	35.9	10.0	-22.3	-25.7	2.53	1.12	421	953	319	394	443
PU-8000-70	53.9	33.1	4.5	-19.4	-22.2	1.43	1.40	736	752	325	403	451

data obtained for polyurethanes prepared in this study, the PU-3000-50, PU-8000-50, and PU-8000-60 films had the lowest chain mobility due to the lowest peak heights (Figure 10). This result can be evaluated together with XRD and DSC results that among all samples the crystallinity of the related samples had the highest value. Thus, the crystalline phases acted as barriers for polymer chains against moving under applying force in DMA measurements.

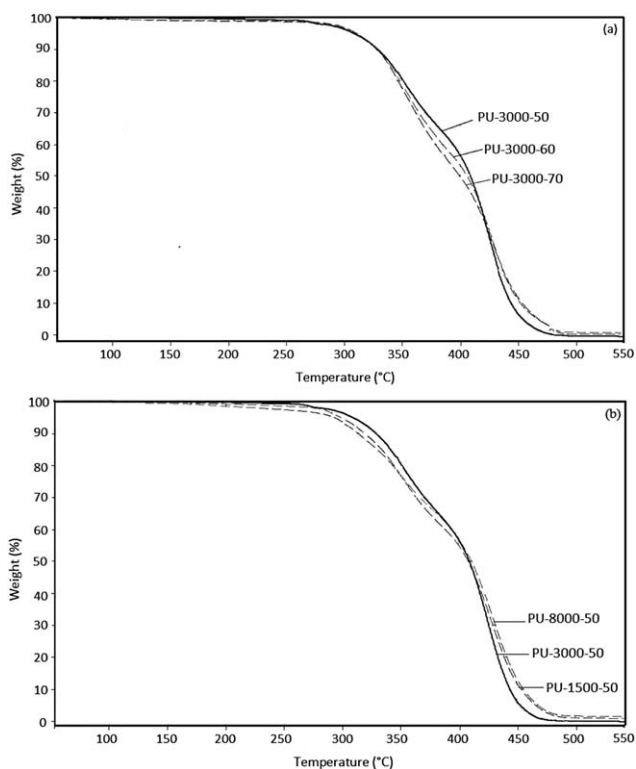
Crosslink Density and Average Molecular Weight Between Two Crosslinks

Both chemical and physical crosslinks are very important factors on some properties of polyurethanes including shape memory property. Generally, two methods are used for determination of crosslink density; namely the equilibrium swelling and the rubber elasticity methods.²⁸ The data obtained by the equilibrium swelling method according to Flory-Rehner equation are evaluated for an explanation of the effect of the chemical crosslinks. On the other hand, total crosslinks (physical and chemical crosslinks) can be determined by the rubber elasticity method using DMA data. Thus, the effects of physical crosslinks can be emphasized with evaluating data together obtained from two methods.

For the polyurethane films prepared in this study, crosslink density (v_c) and average molecular weight between two crosslinks (M_c) estimated accordingly by two methods are given in Table I. As expected, the crosslink density determined by the equilibrium swelling method decreased with increasing both the amount and the molecular weight of PEG in polyurethane structure. In other words, the crosslink density decreased with decreasing HSC for the PEG 3000-based polyurethanes, and with increasing SSL for the polymers prepared with a 50 : 50 ratio of CO and PEG. The average molecular weight between two crosslinks is inversely proportional to crosslink density.

Since total of the chemical and physical crosslinks can be determined by the rubber elasticity method,²⁹ the crosslink density calculated from DMA curves should be higher than those

obtained by the equilibrium swelling method. Additionally, it is expected that increasing castor oil content in polymer structure (increasing CO : PEG ratio) should also increase crosslink density. The unexpected results were obtained for the polymers prepared in this study. This may be due to the existence of the dangling chains origin from castor oil. The dangling chains may act as plasticizer, thus lowering the E' value which was used for calculation of M_c and v_c . The similar explanation was reported for the triolein-based polyurethane networks by Zlatanovic et al.²⁹ It was pointed out that the plasticizing effect of dangling chains

**Figure 7.** TGA curves of polyurethane films.

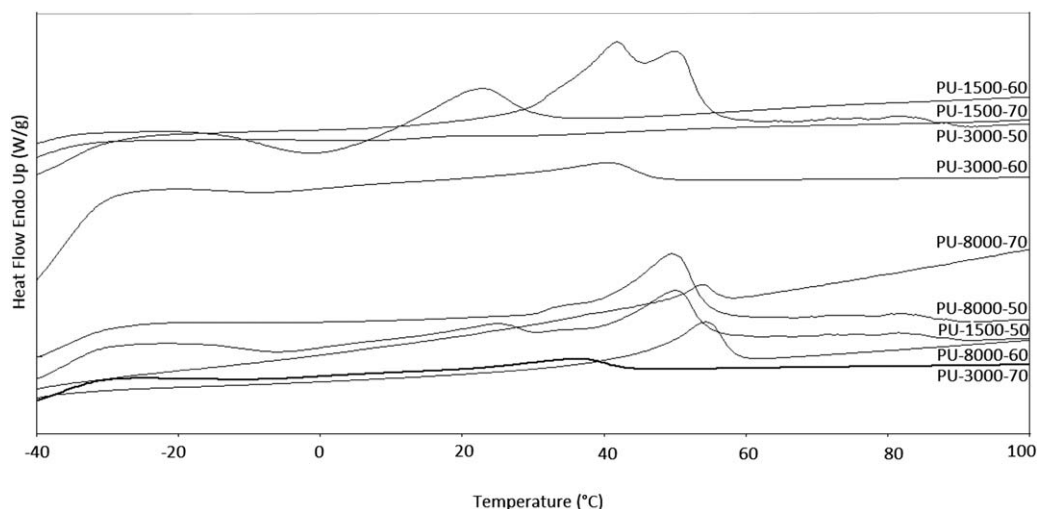


Figure 8. DSC curves of polyurethane films.

in polymer network. From these results it is assumed that the rubber elasticity method is not suitable for determination of M_c and ν_c of the polymers prepared in this study.

Shape Memory Properties

Shape memory property was not observed for the polymers when the ratio of CO : PEG was higher than 70 : 30 in polymer synthesis. Since it is not possible to prepare polymers lower than 50 : 50 of CO:PEG ratio due to their poor mechanical properties, the polyurethanes with 50 : 50, 60 : 40, and 70 : 30 ratio were prepared and their shape memory properties were investigated.

It is well known that SSL, HSC, crosslink density, glass transition/melting temperature, and crystallinity play very important roles in the shape memory behavior of the polymers.^{10,30} Generally, the effects of these parameters are investigated in a series of experiments. In this study, the influences of all these parameters on shape memory properties were also investigated. The experiments were performed at constant SSL with varying HSC. Crosslink density, T_g and crystallinity of each polymer were

highly depended on the ratio of CO to PEG and the molecular weight of PEG.

The shape fixity and shape recovery rates (R_f and R_r , respectively) given in Table II, are the average values of six measurements. As shown, both of them increased with decreasing HSC for two cooling rates. Among PEG 3000-based polyurethanes, the highest R_f and one of the highest R_r were obtained for PU-3000-50 which has one of the highest crystallinity, and one of the lowest HSC and crosslink density (Figure 6 and Table I). The lowest R_f and R_r were obtained for the PU-3000-70-coded polymer which is amorphous structure and contains the lowest PEG. Although PU-3000-60 and PU-3000-50-coded polymers have the same SSL, different shape fixity rates were obtained for each one, due to the differences in their crosslink densities and HSC. The similar results are reported by other researchers.^{10,30,31} In fact, the crystallinity, HSC and crosslink density were related to each other, and all of them depended on the CO : PEG ratio and the molecular weight of PEG. Taking into account the shape memory properties of all polymers the optimum properties were achieved in the case of PU-3000-50.

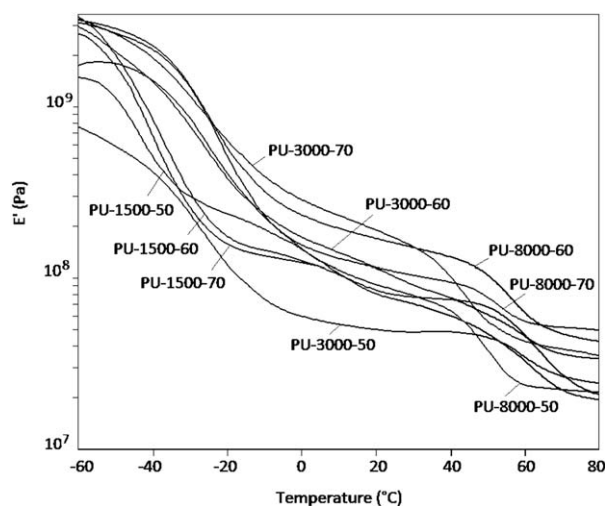


Figure 9. Storage modulus of polyurethane films.

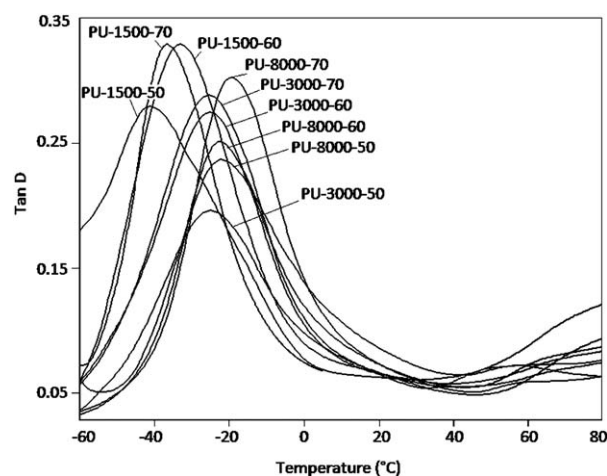


Figure 10. Tan D of polyurethane films.

Table II. Shape Memory Properties of Polyurethane Films

Code	R_f (%) at:		R_r (%) at:		
	Low cooling rate ^a	High cooling rate ^b	Low cooling rate ^a	High cooling rate ^b	High cooling rate ^c
PU-1500-50	83.1	89.8	94.1	96.7	61.7
PU-1500-60	76.0	81.3	93.1	94.1	41.4
PU-1500-70	50.1	61.1	82.0	88.7	76.2
PU-3000-50	90.6	92.3	93.9	96.3	87.8
PU-3000-60	66.8	68.5	88.3	91.8	61.5
PU-3000-70	47.8	57.4	84.1	88.6	78.3
PU-8000-50	94.6	97.7	92.6	94.0	13.3
PU-8000-60	90.1	93.4	91.6	92.0	31.0
PU-8000-70	71.7	84.5	87.6	91.7	42.7

^a Deformation at 65°C, shape fixity at 25°C, and shape recovery at 65°C in air.

^b Deformation at 65°C, shape fixity at 5°C, and shape recovery at 65°C in air.

^c Deformation at 65°C, shape fixity at 5°C and shape recovery at 37°C in PBS.

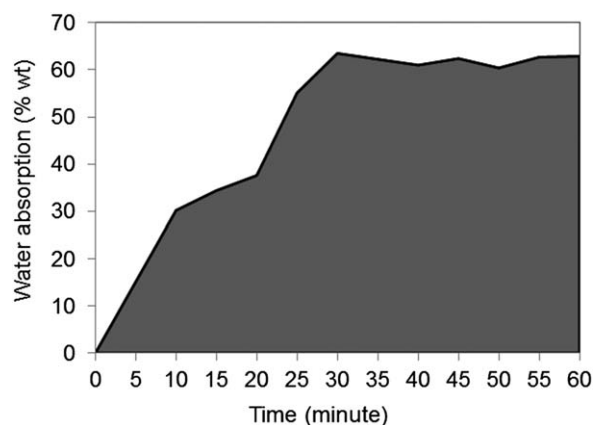
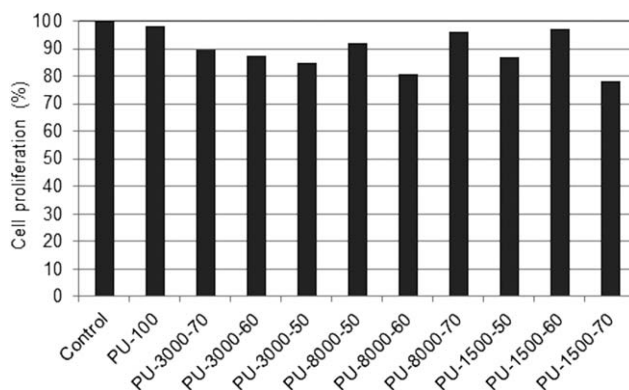
Table III. Density, Swelling Ratio, Gel Content, Water Contact Angle, and Surface Free Energy of Polyurethane Films

Code	SSL (g/mol)	HSC (%)	Density (g/cm ³)	Swelling ratio (%)	Gel content (%)	Water contact angle (°)	Surface free energy (mN/m)
PU-1500-50	1500	65.5	1.0835	34	90	69	41.1
PU-1500-60		72.9	1.0765	29	93	72	39.4
PU-1500-70		80.1	1.0616	18	96	76	36.6
PU-3000-50	3000	63.7	1.0812	67	82	61	49.4
PU-3000-60		71.9	1.0735	42	78	65	45.8
PU-3000-70		79.6	1.0504	24	94	70	37.7
PU-8000-50	8000	62.5	1.0702	70	69	51	56.3
PU-8000-60		71.1	1.0657	61	69	54	52.2
PU-8000-70		79.2	1.0499	39	71	56	51.3

Since hard and soft segments independently affect the shape recovery rate, not only the correlation between the R_f and independent variables, but also the effect of the interaction of HSC and SSL were sought with eq. (10),

$$R_r = a(\text{SSL}) + b(\text{HSC}) + c(\text{SSL})(\text{HSC}) \quad (10)$$

where a , b , and c are the coefficients. For calculations the data obtained at high cooling rate in programming step were used. The coefficients a , b and c were calculated as 0.0404, 1.5404,

**Figure 11.** The swelling kinetic data of the PU-3000-50.**Figure 12.** Proliferation of NIH 3T3 cells on polyurethane films (MTT assay results).

and -6.5×10^{-4} , respectively. Since the coefficient of the HSC, b , is greater than the others, it can be concluded that the HSC is the significant parameter on shape recovery rate for the polyurethanes synthesized in this study.

It is well known that if the transition temperature is a melting point, the shape memory properties of the polymer are influenced by programming parameters such as the cooling rate, the lowest temperature (T_{low}) in cooling step and the time period when the sample is held at T_{low} .³² In order to determine the effect of programming parameters on shape memory behavior of the polymers prepared in this study, the bending test was applied in two different temperature ranges; high (from 65 to 5°C, $\Delta T = 60$) and low (from 65 to 25°C, $\Delta T = 40$) temperature ranges. Thus, either cooling rate or T_{low} could be changed. It was found that the high temperature difference for fixing temporary shape caused to increase shape fixity and shape recovery rates. The shape recovery rate is relatively low in PBS medium at 37°C for all polymers. The best result was obtained for PU-3000-50 (Table II).

Six consecutive measurements were done by bending test in order to determine repeated use of each sample as shape memory material. The maximum decrease in performance of the films was 2% after 6th cycle. The crystallinity of the samples was determined by DSC after fixing and after shape recovery. It was found that fixing and recovery have no effect on the crystallinity of the prepared PU samples.

Density, Swelling Ratio, Gel Content, and Surface Free Energy

Density, swelling ratio and gel content of the polymers are given in Table III. Density of the polyurethanes tended to decrease with increasing CO content. The gel content increased with decreasing SSL.

The swelling ratio of the polymers depended on both HSC and SSL; increased with decreasing HSC but decreased with decreasing SSL. The swelling kinetic data of the PU-3000-50 which shows the optimum properties and shape memory performances are shown in Figure 11. As can be seen, the film took 30 min to reach an equilibrium.

Water contact angle and surface free energy of the polymers are given in Table III. Water contact angle is proportional to HSC due to the hydrophobic structure of castor oil, and inversely proportional to SSL due to hydrophilic structure of PEG. It is well known that, water contact angle is inversely proportional to surface free energy.

Cytotoxicity of Polyurethane Films

The results of the MTT test indicated, in general, that the polymers did not demonstrate any cytotoxicity. Each of them had a proliferation ratio of more than 80% when MTT test was used with NIH 3T3 cells (Figure 12). The PU-100 has the maximum proliferation ratio, which is very close to the positive control.

When the direct contact test was used for determination of cytotoxicity, morphological observations revealed cells with normal morphology, spreading, and growing to confluency on all types of surfaces, but not the series of PU-8000. The PU-100

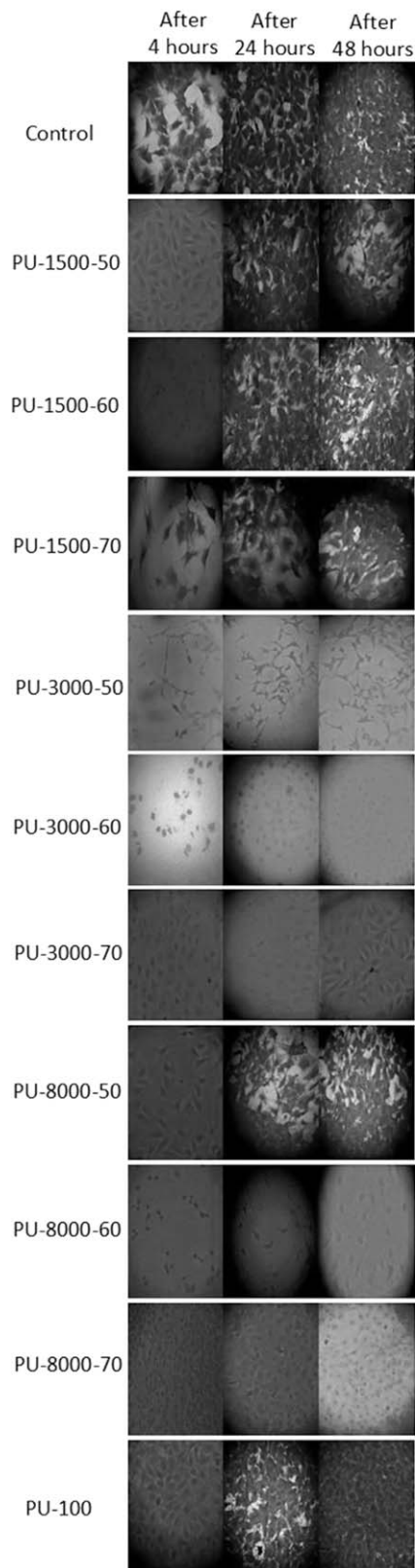


Figure 13. Images of the NIH 3T3 cells attached on the surface of the polyurethane films.

has the most similar morphological image to the control (Figure 13). Spreading on the surface of the polymer series of PU-1500 was much more than the others and did not induce changes in

the cell morphology. The maximum spreading was observed on the surface of PU-3000-50 in the series of the PU-3000. When the series of PU-8000 were examined, they induced changes in the cell morphology and adhesion of fibroblasts exposed to the polymers. There were fewer cells attached to surfaces.

CONCLUSIONS

Polyurethane hydrogels were successfully synthesized from castor oil, which is natural polyol, and polyethylene glycol in different SSL and HSC. Thus, polyurethanes having various crystallinity, density, hydrophilicity, swelling ratio, melting, and glass transition temperatures, and crosslink density were obtained, and their physical and shape memory properties could be correlated to their chemical structure. The main results of the study can be resumed in the following items:

1. The crystallinity, swelling ratio, surface free energy, melting temperature, and average molecular weight between two crosslinks of the polymers increased by decreasing HSC and increasing SSL.
2. The shape memory properties of polyurethanes were determined by bending test applied at two different cooling rates in programming step. Improved shape memory properties were obtained at high cooling rate.
3. The shape memory properties were closely related to the HSC. The polyurethane prepared with relatively low HSC, showed improved shape memory behavior.
4. According to the R_f and R_r results, optimum amount of castor oil in polyurethane structure was suggested as 50% (by weight) of total polyol component. After taking T_m values of the polymers into account PU-3000-60 and PU-3000-50 films can be used in biomedical applications, since their T_m are close to human body temperature. All results indicate that PU-3000-50-coded polyurethane has a high potential as shape memory biopolymer.
5. The polymers did not exhibit cytotoxicity.

REFERENCES

1. Behl, M.; Lendlein, A. *Mater. Today* **2007**, *10*, 20.
2. Chun, B. C.; Cho, T. K.; Chong, M. H.; Chung, Y. C. *J. Mater. Sci.* **2007**, *42*, 9045.
3. Cao, Q.; Chen, S.; Hu, J.; Liu, P. *J. Appl. Polym. Sci.* **2007**, *106*, 993.
4. Baer, G.; Wilson, T. S.; Matthews, D. L.; Maitland, D. J. *J. Appl. Polym. Sci.* **2006**, *103*, 3882.
5. Lin, J. R.; Chen, L. W. *J. Appl. Polym. Sci.* **1998**, *69*, 1563.
6. Zhu, Y.; Hu, J.; Liu, Y. *Eur. Phys. J. E* **2009**, *28*, 3.
7. Tobushi, H.; Matsui, R.; Hayashi, S.; Shimada, D. *Smart Mater. Struct.* **2004**, *13*, 881.
8. Gultekin, G.; Oral, C. A.; Erkal, S.; Sahin, F.; Karastova, D.; Tantekin-Ersolmaz, S. B.; Guner, F. S. *J. Mater. Sci. Mater. M* **2009**, *20*, 421.
9. Yücedag, F.; Oral, C. A.; Erkal, S.; Sirkecioglu, A.; Karasartova, D.; Sahin, F.; Tantekin-Ersolmaz, S. B.; Güner, F. S. *J. Appl. Polym. Sci.* **2010**, *115*, 1347.
10. Li, F.; Larock, R. C. *J. Appl. Polym. Sci.* **2002**, *84*, 1533.
11. Lippincott, H. W. Development and Characterization of a Family of Shape Memory, Biocompatible, Degradable, Porous (co)-polyurethanes via Sol-gel Chemistry. PhD Thesis, University of Massachusetts Lowell, U.S., **2009**.
12. Rio, E. D.; Lilligadas, G.; Ronda, J. C.; Galia, M.; Meier, M. A. R.; Cadiz, V. *J. Polym. Sci. Polym. Chem.* **2011**, *49*, 518.
13. Ping, P.; Wang, W.; Chen, X.; Jing, X. *Biomacromolecules* **2005**, *6*, 587.
14. Ahmad, M.; Luo, J.; Xu, B.; Purnawali, H.; King, P. J.; Chalker, P. R.; Fu, Y.; Huang, W.; MirafTAB, M. *Macromol. Chem. Phys.* **2011**, *212*, 592.
15. Cheetham, N. W. H.; Tao, L. *Carbohydr. Polym.* **1998**, *36*, 277.
16. Brandrup, J.; Immergut, E. H.; Grulke, E. A. *Polymer Handbook*, 4th ed.; Wiley: New Jersey, **1999**; Vol. 2.
17. Hill, L. W. In *Paint and Coating Testing Manual 14th edition of the Gardner-Sward Handbook*; Koleske, J. V., Ed.; Ann Arbor, MI: ASTM Manual Series: MNL 17, **1995**.
18. Hu, J. *Shape Memory Polymers and Textiles*; CRC Press: Cambridge, **2007**.
19. Akkas, T.; Citak, C.; Sirkecioglu, A.; Güner, F. S. *Polym. Int.* **2013**, *62*, 1202.
20. Oprea, S. *Polym. Bull.* **2010**, *65*, 753.
21. Karak, N.; Rana, S.; Cho, J. W. *J. Appl. Polym. Sci.* **2009**, *112*, 736.
22. Oprea, S. *J. Am. Oil Chem. Soc.* **2010**, *87*, 313.
23. Coleman, M. M.; Lee, K. H.; Skrovanek, D. J.; Painter, P. C. *Macromolecules* **1986**, *19*, 2149.
24. Oprea, S. *J. Mater. Sci.* **2011**, *46*, 2251.
25. Hablot, E.; Zheng, D.; Bouquey, M.; Averous, L. *Macromol. Mater. Eng.* **2008**, *293*, 922.
26. Joykumar Singh, T. H.; Bhat, S. V. *Bull. Mater. Sci.* **2003**, *26*, 707.
27. Menard, K.P. *Dynamic Mechanical Analysis: A Practical Introduction*, 1st ed.; CRC Press: Boca Raton, **1999**.
28. Yeganeh, H.; Talemi, P. H. *Polym. Degrad. Stabil.* **2007**, *92*, 480.
29. Zlatanovic, A.; Petrovic, Z. S.; Dusek, K. *Biomacromolecules* **2002**, *3*, 1048.
30. Lee, S. H.; Kim, J. W.; Kim, B. K. *Smart Mater. Struct.* **2004**, *13*, 1345.
31. Chen, S.; Hu, J.; Liu, Y.; Liem, H.; Zhu, Y.; Liu, Y. *J. Polym. Sci. Polym. Phys.* **2007**, *45*, 444.
32. Lendlein, A.; Kelch, S. *Angew. Chem. Int. Ed.* **2002**, *41*, 2034.